EFFECT OF CORE FLOW HEAT TRANSFER ENHANCEMENT ON POWER GENERATION CHARACTERISTICS OF THERMOELECTRIC GENERATORS WITH DIFFERENT PERFORMANCES

by

Yanzhe LI[a,b]***, Shixue WANG***[a,b*]***, Yunchi FU***[c]***, Yulong ZHAO***[a,b]***, and Like YUE***[a,b]

[a] School of Mechanical Engineering, Tianjin University, Tianjin, China
[b] Key Laboratory of Efficient Utilization of Low and Medium Grade Energy, Ministry of Education, Tianjin University, Tianjin, China
[c] Intelligent Manufacturing College, Tianjin Sino-German University of Applied Sciences, Tianjin, China

Original scientific paper
https://doi.org/10.2298/TSCI210309184L

In this study, the effect of enhancing the core flow heat transfer with metal foam on the performance of thermoelectric generators with different power generation characteristics is studied experimentally. Filling the core flow area of the gas channel in a thermoelectric generator with metal foam can greatly improve the heat transfer capacity of the gas channel with a small pressure loss, thereby improving the power generation efficiency. The results show that, first, the heat transfer enhancement achieved by partially filling the core area of the gas channel with metal foam can significantly improve the performance of thermoelectric generators, the maximum output power is about 1.5 times higher than that of the unfilled channel. Second, for a thermoelectric generator with different modules, the friction coefficient for different filling ratios increases by about 16 times at most, while the Nusselt number value increases by only three times at most, and according to the performance evaluation criteria of the gas channel, metal foam with high filling rate and low pore density is more suitable for the thermoelectric generator. Third, it is more appropriate to use the thermoelectric module with a high figure of merit as the selection criterion for deciding whether to adopt the technique of enhancing heat exchange through the gas channel. The maximum output power and efficiency of the thermoelectric generator using the high figure of merit module are 300% and 160% higher than those of the thermoelectric generator using the low figure of merit module, respectively.

Key words: *thermoelectricity, heat-transfer enhancement, metal foam, thermoelectric module, core flow*

Introduction

As solid-state energy conversion device, thermoelectric generators can directly convert thermal energy into electrical energy. However, due to the limitations of the performance of thermoelectric materials and heat source conversion modes, the energy conversion efficiency of thermoelectric generators is low, which restricts the extent of their applications. Investigations into thermoelectric power generation technology has a long history. Scholars

* Corresponding author, e-mail: wangshixue_64@tju.edu.cn

have performed considerable research on the application of thermoelectric technology to medical [1], industrial [2], civil fields [3], and space exploration and the military [4], as well as to engine technologies. About 30-40% of the fuel energy in vehicles with internal combustion engines (ICE) is released into the atmosphere as waste heat energy [5]. The CO_2 unburned hydrocarbons (UHC), CO, NO_x, and particulate matter (PM) emitted into the atmosphere by internal combustion engines will cause environmental and health hazards [6-8]. The engine efficiency could be increased by approximately 4-5% by converting the exhaust waste heat energy of ICE into useful energy with thermoelectric waste heat recovery systems.

There are many ways to improve the performance of the thermoelectric generator, such as changing the material of the thermoelectric power generation module, changing the working medium used in the thermoelectric generator, and changing the structure of the thermoelectric generator, *etc.* Topalci *et al.* [9] designed a thermoelectric generator using different materials of p-n pairs to recover the exhaust waste heat of internal combustion engines. Four different semiconductor materials of type Bi_2Te_3, $Bi_{0,3}Sb_{1,7}Te_3$, $PbSe_{0,5}Te_{0,5}$, and Zn_4Sb_3 were used in the thermoelectric generator. The results showed that the p-n pairs of the thermoelectric modules made by $Bi_{0,3}Sb_{1,7}Te_3$, and Bi_2Te_3 type semiconductors produce the highest output power. Also, using the thermoelectric generator created by connecting twenty thermoelectric modules in series, 86.53 W DC electrical power was obtained by the temperature difference 162.4 K at 4000 rpm engine speed. Ge *et al.* [10] studied the cold energy thermoelectric power generation. Liquid nitrogen was used as cryogenic liquid in the experiment, the thermoelectric characteristics of the system were studied experimentally. The results revealed that in the liquid-phase and two-phase regions, the temperature difference between the hot and cold sides increased in the gasification process. However, in the gas-phase region, it first decreased and then increased. The temperature difference between the hot and cold module sides was small, being only 7.2-28.1 °C. For a thermoelectric generator that uses gas as the heat source fluid, the cold side is usually cooled by water, and the heat transfer coefficient is generally higher than 1000 W/m^{2}K. In contrast, the effective heat transfer coefficient of exhaust gas flowing along the heat exchanger on the hot side is typically only 20-80 W/m^{2}K [11]. Therefore, the main effect of heat transfer in a thermoelectric generator is to increase the heat transfer on its hot side. The heat transfer efficiency can be improved by simply modifying an ordinary heat exchanger. One way of conveniently accomplishing this task is to add interpolation in the channel. For example, Liu *et al.* [12] compared two kinds of flat plate type automobile exhaust thermoelectric generators with different fins, and found that the output power of the channel using the chaos type fins increased by 14.4% compared with the channel using the fishbone type fins. Byung *et al.* [13], respectively, arranged three spoiler elements of rectangular column, upwind triangular column and leeward triangular column in the tail gas channel of the thermoelectric generator. It was found that the power generation performance of the thermoelectric generator equipped with rectangular column was up to 6.2 W, and the output power of the other two triangular columns was about 5.5 W. Lu *et al.* [14] experimentally compared the effects of uniform distribution and non-uniform distribution of vortex generators in the exhaust channel on power generation performance. The results showed that non-uniform distribution can obtain higher output power. Compared with smooth channel, the output power is increased by 177.4% and the power generation efficiency can reach 1.2%. Wang *et al.* [15], respectively, set cylindrical grooves and interpolated fins in the square exhaust gas channel. The results showed that the grooves not only make the output power of the system larger but also reduce the pressure loss, and when the channel height is 8 mm, the system can obtain the optimal overall performance. In order to reduce the contact thermal resistance between the module and the cold and hot fluid channels, Kim *et al.* [16] designed a thermoelectric power generation system with direct contact exhaust gas. The experimental results showed that the maximum output power of the system is 43 W, and the power generation efficiency reaches 2%. The calculation showed that compare with the traditional thermoelectric power generation system, the maximum output power is increased by 132%, and the pressure drop is reduced by 23%. The insertion of porous material can greatly improve the effective thermal conductivity of the fluid in the channel. In particular, porous foam material is a type of high performance interpolation that can enhance the heat transfer inside the channel. It has three main advantages. First, its internal structure is complex, which makes the fluid flow through its pores more non-linear. This increases the disturbance to the fluid, thus promoting the heat exchange between the surface of the solid skeleton and the fluid. Second, the specific surface area of the porous foam is large, which maximizes the contact area per unit volume between the solid skeleton and the fluid. Thirdly, the solid skeleton of porous metal foam is a good conductor of heat and has a high thermal conductivity. These beneficial characteristics have motivated scholars to conduct detailed investigations on how heat transfer can be enhanced by porous media inserted into the channel.

For example, Megerlin *et al.* [17] carried out an experimental study on the circular channel using mesh and brush inserts made of stainless steel-woven wires. The experimental results showed that both of the two kinds of inserts exerted a positive effect on the heat transfer in the channel, and the mesh insert had the most effect. Wang *et al.* [18] carried out a numerical simulation and experimental studies on the characteristics of the heat transfer and pressure drop with a filament insert into a square channel. Both numerical and experimental results showed that an increase in heat transfer led to a very small decrease in pressure drop when using the filament insert. Pavel and Mohamad [19] carried out an experimental study on the pipe using porous inserts consisting of wire mesh. The experimental results showed that the high porosity of the porous medium could effectively improve the heat transfer in the pipe. For instance, porosities of 98.1% and 99.3% lowered the pressure in the pipe to 64.8 Pa and 19.1 Pa, respectively. Thus, the high porosity of the porous media caused only a small pressure drop inside the pipe. Although the insertion of the metal wire can enhance the heat transfer, because of the small contact area between the wire and the gas, the effect on the heat transfer is limited. Therefore, scholars have considered filling the channel with metal foam to enhance the gas heat transfer in the channel. Hsieh *et al.* [20] carried out an experimental study on a rectangular channel full filled aluminum foam inserts, and discussed the influence of the porosity and pore density of the metal foam on the heat transfer characteristics of the channel. The results showed that the Nusselt number increases as the pore density and porosity of the porous foams increase. Boomsma *et al.* [21] conducted an experimental study in which aluminum foam was used for performance enhancement of heat exchangers. The results showed that the aluminum foam could effectively improve the heat transfer capability of the heat exchanger. Pavel and Mohamad [22] and Mohamad 23] compared the heat transfer characteristics of a circular channel fully filled with a porous medium and at the core flow area filled with a porous medium. When the filling ratio of the porous medium was 1, the temperature uniformity of the flow field in the channel was weaker than that for the filling ratios of 0.4 and 0.6. The numerical simulation by Wei and Yang [24] showed that it was very effective in enhancing the heat transfer performance of the channel wall by filling with a porous medium with high thermal conductivity and high porosity at the core flow area of the channel. Huang *et al.* [25] used the porous medium of a copper screen (the pore density of which is 10 PPI and the porosity of which are 0.951, 0.966, and 0.975, respectively) to partially fill the core of a circular channel to enhance the heat transfer. Both the numerical and experimental results showed that the convective heat transfer was considerably enhanced by the porous inserts in the channel and the corresponding flow resistance was increased by a moderate extent. The filling of metal foam can make the temperature distribution in the core flow area of the channel more uniform. Furthermore, the velocity gradient near the channel wall increased as the filling ratio increased, which can effectively improve the heat transfer rate. Zheng *et al.* [26] conducted a numerical simulation study of the effect of convective heat transfer in a circular channel by inserting porous media (porosities 0.9726, 0.9546, 0.9486, and 0.9272 and pore densities 5 PPI, 20 PPI, 10 PPI, and 40 PPI) in the core flow area by numerical methods. In most cases, the Nusselt number and the performance evaluation criteria (PEC) decreased as the porosity of the foamed metal increased. For all heat transfer enhancement conditions, the Nusselt number increased as the Reynolds number increased, but the PEC decreased as Reynolds number increased. In the previous experimental study, in Hixon [1] author discussed the effect of the enhancement of core flow heat transfer on the performance of thermoelectric generators. The results showed that the heat transfer coefficient of the surface of the gas channel wall in the thermoelectric generator can be increased by filling the channel with metal foam. As a result, the output power of the thermoelectric generator can be improved.

Despite these positive results, the effect of the performance of different thermoelectric modules should be different for the same heat transfer enhancement mode due to the different figures of merit, thermal resistance, and seebeck coefficients for different thermoelectric modules. However, this has not been investigated. Therefore, on the basis of previous research [27], this study adopts thermoelectric modules with different performances, and experimentally examines the effects of enhancing core flow heat transfer on the power generation characteristics of thermoelectric generators for the same heat transfer conditions.

Introduction of experimental device

Figures 1(a) and 1(b) are 2-D and 3-D drawings of the thermoelectric generator, respectively. As shown in the figures, the core flow area of the gas channel in the experimental

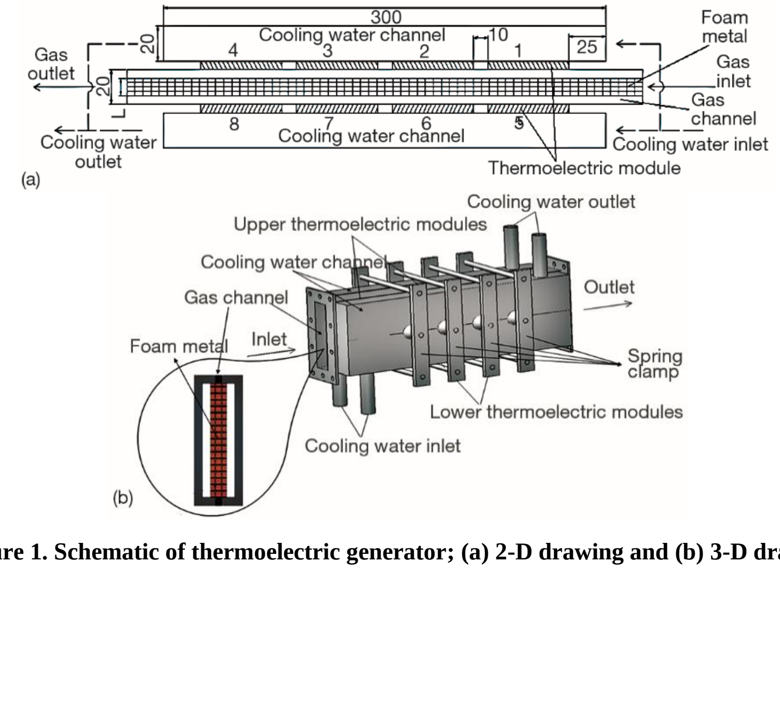

Figure 1. Schematic of thermoelectric generator; (a) 2-D drawing and (b) 3-D drawing

thermoelectric generator is partially filled with copper foam. On the one hand, its high thermal conductivity and temperature uniformity improve the heat exchange capacity of the fluid in the channel. On the other hand, since the filling is incomplete, it is expected to effectively suppress a decrease in pressure. The basic parameters of the thermoelectric module used in the experiment are shown in tab. 1, and the structural size of the thermoelectric generator is shown in tab. 2. The experiment is divided into five cases, and the basic conditions for each case are listed in tab. 3. The wall thicknesses of the gas channel and the cooling water channel were both 5 mm. For details of the experimental system, see [27].

Table 1. Basic parameters of different thermoelectric module

	Length [mm]	Width [mm]	Height [mm]	Specific conductance, σ [sm^{-1}]	Thermal conductivity, k [Wm^{-1}K^{-1}]	Seebeck coefficient, α [VK^{-1}]	Figure of merit ZT [–]
TEHP1-12656-0.3	56	56	5	2.75	1.12	0.030	0.66
KTGM199-2	56.5	48	1.36	0.12	0.12	0.068	1.39
KTGM161-18	55	51.5	4.4	0.78	0.48	0.058	1.64

Table 2. Structure size of the thermoelectric generator

	Length [mm]	Width [mm]	Height [mm]	Wall thickness [mm]
Interior of the gas channel	350	70	20	5
Interior of the cooling water channel	300	70	20	5

Table 3. Basic conditions of each case

	Case 0	Case 1	Case 2	Case 3	Case 4
PPI	0	20	40	20	40
Porosity	0	98%	98%	98%	98%
Filling rate	0	50%	50%	75%	75%

Experimental system

The experimental system is shown in fig. 2. First, the air output by the air compressor is sent to the regenerator after passing through the pressure stabilizing tank. Then, the air preheated in the regenerator enters two sets of heaters for heating. The heated high temperature air enters the thermoelectric generator for thermoelectric conversion. The high temperature exhaust gas from the generator enters the heat regenerator, and heat exchange with the air from the air compressor occurs, which is then discharged outside. The arrangement of the heat regenerator increases the room temperature before air enters the heater. It reduces the power rating of the heater and saves energy for heating.

The input and output temperatures of the generator, and the hot and cold side temperatures of the thermoelectric module are measured in real time using a thermocouple (K-type thermocouple, precision ±0.1 °C). A data-acquisition instrument is used to record the temperature and voltage of the module. The air and cooling water flows are measured using a flowmeter (gas flowmeter DY025: Range 15-200 m^3/h, precision ±1.5%; fluid flowmeter

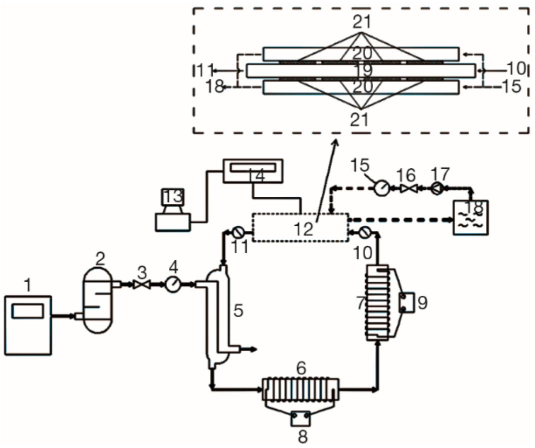

Figure 2. Experimental system diagram;
1 – air compressor, 2 – gasholder, 3 – throttle, 4 – gas flowmeter, 5 – heat regenerator, 6. – heater, 7 – heater, 8 – voltage regulator, 9 – voltage regulator, 10 – pressure gage, 11 – pressure gage, 12 – thermoelectric generator, 13 – PC, 14 – data acquisition instrument, 15 – fluid flowmeter, 16 – throttle, 17 – pump, 18 – cooling water tank, 19 – gas channel, 20 – cooling water channel, and 21 – thermoelectric module

AXF015G: Range 0.1-15 m/s, precision ±0.5%). The inlet and outlet of the generator is equipped with pressure gauges (TRD-3051GP5E22M3B3: Range 0-17.24-690 kPa, precision ±1.0%) to measure the pressure and to calculate the pressure difference.

System reliability and error analysis

The reliability and measurement error of the experimental results were tested in the previous study, for details see [27]. The equations used is:

$$h=\frac{c\dot{m}(T_{\text{in}}-T_{\text{out}})}{A\left[\dfrac{(T_{\text{in}}+T_{\text{out}})}{2}-\dfrac{c\dot{m}(T_{\text{in}}-T_{\text{out}})\delta}{\lambda A}-\overline{t}_{\text{w}2}\right]} \tag{1}$$

where h is the wall heat-transfer coefficient, c – the gas specific heat, $\dot{m}$ – the gas mass flow, T_{in} – the gas inlet temperature, T_{out} – the gas outlet temperature, δ – the wall thickness, λ – the thermal conductivity of the channel wall, A – the heat exchange area, and $\overline{t}_{\text{w}2}$ – the outside wall average temperature of the gas channel.

$$\text{Re}=\frac{\rho uD}{\mu} \tag{2}$$

$$\text{Nu}=\frac{hD}{\lambda_{\text{g}}} \tag{3}$$

$$f=\frac{2D\Delta p}{L\rho u^2} \tag{4}$$

where Re is the Reynolds number, Nu – the Nusselt number, f – the friction coefficient, ρ – the gas density, u – the gas velocity, D – the equivalent diameter, μ – the gas viscosity, λ_{g} – the gas thermal conductivity, Δp – the pressure drop of the gas channel, and L – the length of the gas channel.

$$\sigma h=\left[\left(\frac{\partial h}{\partial \dot{m}}\sigma\dot{m}\right)^2+\left(\frac{\partial h}{\partial T_{\text{in}}}\sigma T_{\text{in}}\right)^2+\left(\frac{\partial h}{\partial T_{\text{out}}}\sigma T_{\text{out}}\right)^2+\left(\frac{\partial h}{\partial \overline{t}_{\text{w}2}}\sigma\overline{t}_{\text{w}2}\right)^2\right]^{1/2} \tag{5}$$

where σ is the maximum error of each measurement parameter.

As shown in [27], through the repeated experiments, the results of the two experiments under the same experimental conditions are basically consistent, and the error is less than 4%, and the measurement error of h is less than 5.2% by calculation, so the error of Nusselt number can also be considered to be within 5.2%. Therefore, it can be considered that the experimental results are reliable.

Experimental results and analysis

Influence of core flow heat transfer enhancement on the performance of TEG

In this paper, the TEHP1-12656-0.3 module was used to carry out the experimental measurements for five different heat transfer conditions, labeled as Cases 0-4. The inlet parameters of flow rate and temperature were 120 m^3/h and 300 °C, respectively. Figures 3(a)-3(d) show the characteristic power curves of the thermoelectric generator, the changes in Nusselt number, the friction coefficient f, and the PEC in the gas channel, respectively, for different cases.

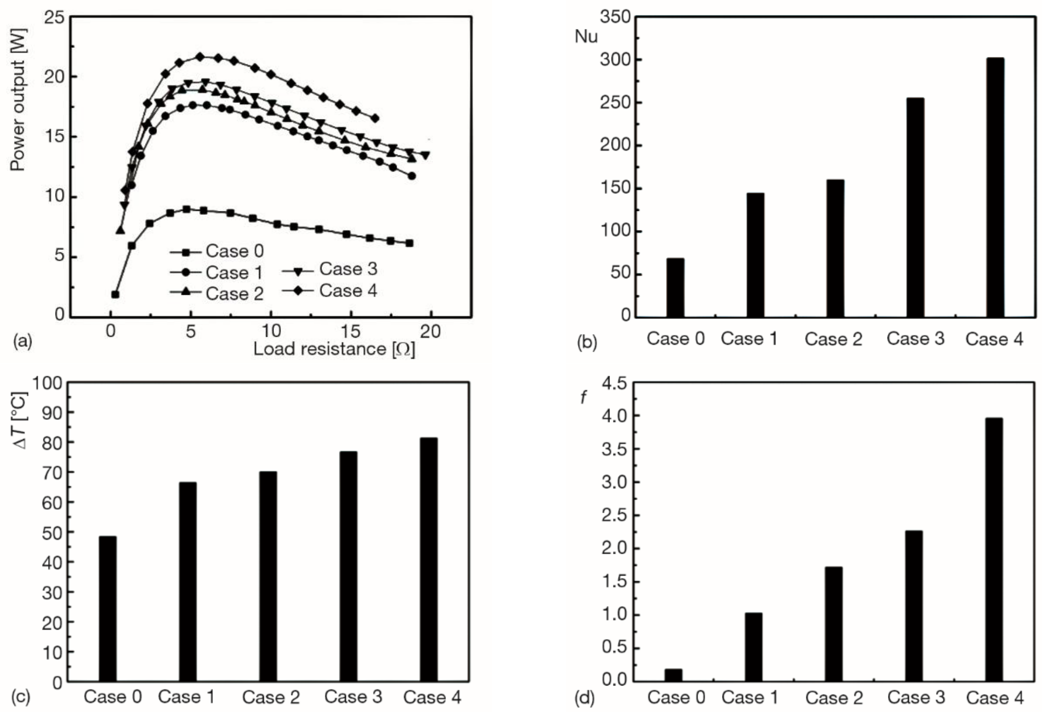

Figure 3. Heat transfer conditions (Cases 0-4); (a) power generation, (b) Nusselt number, (c) temperature difference, ΔT, and (d) friction coefficient, f

As can be seen from fig. 3(a), the output power gradually increases as the loop current increases. When the load resistance is the same as the internal resistance of the thermoelectric generator, the output power reaches the maximum value, beyond which the loop current continues to increase and the output power decreased. Careful observation reveals that there are differences in the external resistance when the maximum power point of each case is reached. That is, the greater the maximum output power, the greater the corresponding external resistance. The reason is that as the maximum output power increases, the temperature difference between the cold side and the hot side also increases. Considering that the cold side is cooled by water, the temperature of the cold side of the module changes only by a small amount. That is to say, the temperature of the hot side of the module increases significantly, which leads to the corresponding increase in internal resistance of the module. Therefore, the external resistance corresponding to the maximum power point increases. Figure 3(a) also indicates that, for cases with enhanced core flow heat transfer, the output power of the thermoelectric generator for Case 4 is the largest, and that of Case 1 is the smallest. This is because the gas encounters more of the metal skeleton when passing through the metal foam with high pore density and high filling rate. This enhances the disturbance, intensifying the turbulence of the gas in the channel, resulting in a higher Nusselt number value for the channel (about twice as high as Case 1). Thus, the heat exchange effect on the hot side is superior, as shown in fig. 3(b). This figure also shows that the influence of the metal foam with different pore densities in the core flow region on the value of Nusselt number in the gas channel of the thermoelectric generator becomes apparent as the filling ratio increases. This is mainly due to an increase in the gas flowing through the metal foam after the filling ratio increases, which leads to the enhancement of the heat transfer caused by the increase in the pore density and the disturbance of the gas. The figure also shows that when the filling rate is 75% (Cases 3 and 4), the influence of the metal foam with different pore densities on the performance of the thermoelectric generator is essentially the same as that of the thermoelectric generator with 50% filling rate (Cases 1 and 2), However, the latter value is higher, and the corresponding maximum output power is about 1.5 times higher than that of the unfilled channel (Case 4). The reason is that as the filling ratio increases, the region with uniform temperature in the core flow area of the channel continuously expands towards the channel wall. Consequently, the temperature gradient near the channel wall increases, a thin fluid layer with more violent temperature changes forms, the gas flow boundary layer near the channel wall becomes thinner, and Nusselt number in the channel maximally increases by more than three times (Case 4). Therefore, the heat exchange effect on the hot side of the thermoelectric generator can be more effectively improved than the cold side. With the improvement of heat exchange effect on the wall surface of the hot side, the temperature difference, ΔT, between the cold and hot sides of the thermoelectric generator also increases. As shown in fig. 3(c), the temperature difference, ΔT, between the cold and hot sides of the thermoelectric generator gradually increases from Case 0 to Case 4. Case 4 is 1.7 times higher than Case 0, which is also the reason why the thermoelectric generator of Case 4 has the highest power generation.

However, for the gas channel on the hot side of the thermoelectric generator, increasing the pore density of the metal foam in the channel or increasing the filling rate leads to an increase in the flow resistance in the channel, as can be seen from fig. 3(d). This figure shows the change in the friction coefficient, f, in the gas channel for the five cases of different heat transfer conditions. For the same filling rate, the friction coefficient increases as the pore density increases. This is because the more dense the skeleton of the metal foam is, the greater the obstruction it creates for the gas flowing through it. Thus, the resistance losses in the channel increase with the density of the metal foam skeleton. In addition, as the filling ratio increases, the output power of the thermoelectric generator also increases, but the magnitude of the increase is much smaller than that of the pressure drop. The friction coefficient for different filling ratios increases by about 16 times at most, while the Nusselt number value shown in fig. 3(b) increases by only three times at most. Therefore, to effectively evaluate the heat transfer enhancement of metal foam filled into the gas channel, not only should the advantage of heat transfer performance be taken into account, but also the disadvantage of flow resistance. The PEC proposed by Webb [28] is normally used to evaluate the comprehensive effect of a heat transfer enhancement mode. The PEC expression is:

$$PEC = \frac{\dfrac{\mathrm{Nu}}{\mathrm{Nu_o}}}{\left(\dfrac{f}{f_o}\right)^{1/3}} \tag{6}$$

where $\mathrm{Nu}/\mathrm{Nu_o}$ is the ratio of the Nusselt number value for the channel filled with metal foam (after heat transfer enhancement) to the Nusselt number value for the smooth channel (before heat transfer enhancement), and f/f_o is the corresponding ratio for the friction coefficient, f.

Figure 4 shows the PEC of the thermoelectric generator for the five cases. Since Case 0 is the reference, its PEC value is 1. The figure shows that the PEC values of Cases 1-4 are all greater than 1, and the PEC value of Case 3 is the highest. The PEC value for a 75% filling rate is greater than that of a 50% filling rate, which shows that filling the gas channel with metal foam is beneficial to the heat transfer enhancement, and a high filling rate generates superior performance. In addition, for the same filling rate, the channels filled with low pore density metal foam have higher PEC values. This shows that for high filling rates and low pore densities, the extent of heat transfer enhancement in the gas channel can compensate for the adverse effects caused by the increase in resistance. Therefore, according to the PEC of the gas channel, metal foam with high filling rate and low pore density is more beneficial to the overall improvement of the heat transfer performance of the channel.

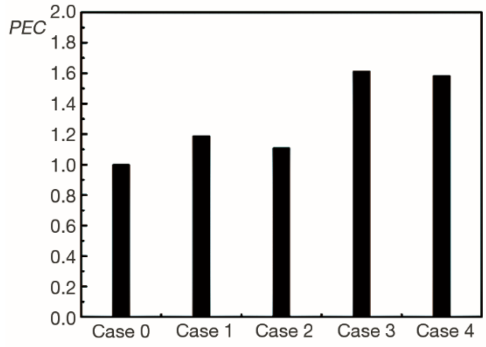

Figure 4. The PEC of the thermoelectric generator

Comparison of power generation performance of different thermoelectric modules

The previous section demonstrated that the performance of a thermoelectric generator filled with metal foam in the core flow region is significantly better than that of an unfilled thermoelectric generator. In order to study the effect of enhanced heat transfer on the power generation performance of thermoelectric modules with different characteristics, three different modules (see tab. 1 for basic parameters) were used for comparative testing in this study.

Figure 5(a) shows a comparison of the output power of the thermoelectric generator for Case 0 for the three modules. As can be seen from the figure, for the same experimental conditions, the thermoelectric generator using the KTGM161-18 module has the highest output power, and the TEHP1-12656-0.3 module has the lowest output power. This is consistent with the figure of merit listed in tab. 1, the higher the figure of merit, the better the power generation performance. For example, the figures of merit for the KTGM161-18 and KTGM199-2 modules are about 2.5 and 2.1 times that of TEHP1-12656-0.3, respectively, and their maximum output powers are about 1.8 and 1.55 times that of TEHP1-12656-0.3, respectively. Therefore, it is very important to use a high performance thermoelectric module to improve the power output of thermoelectric generators. In addition, fig. 5(a) demonstrates that the current density of the maximum power point of each module is different. For example, the current density of the TEHP1-12656-0.3 module (which has smaller resistivity) is the smallest, while the current density of the KTGM199-2 module (which has larger resistivity) is the largest even though its thickness is only 1.36 mm. However, it still has the highest resistance because its resistivity is about 6.5 and 23 times that of KTGM161-18 and TEHP1-12656-0.3, respectively. In addition, the maximum output power of the module is not linear with changes in its thermal resistance for the same cold and hot source temperatures and the same cold and hot side convection heat transfer conditions. This is because the cold and hot side temperature difference in the module depends on the proportional relationship between the module's thermal resistance and the heat transfer resistance on both the cold and hot sides. The output power is also affected by the Seebeck coefficient and the module's resistance. Therefore, the effect of heat transfer enhancement on the hot and cold sides of the module should be different for different modules.

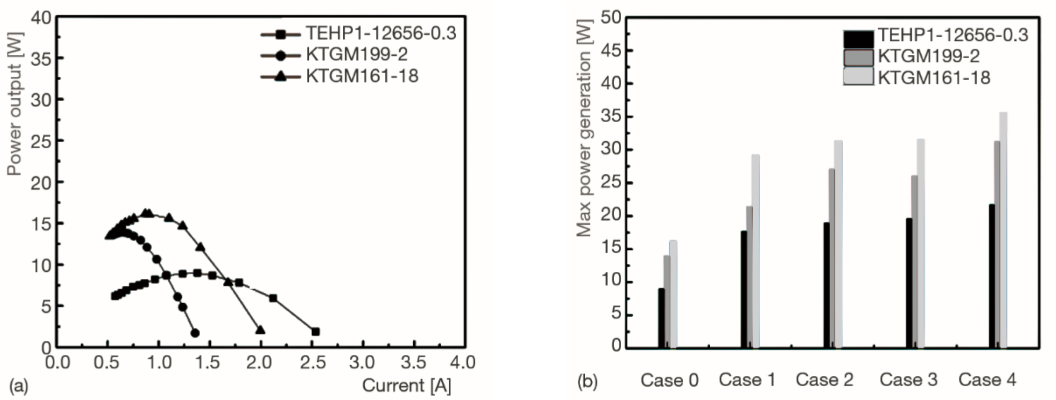

Figure 5. Output power of the thermoelectric generator for Cases 0-4 for the three modules; (a) Case 0 and (b) Cases 0-4

Figure 5(b) shows the comparison between the output powers of the thermoelectric generator for the three modules for Cases 0-4, respectively. Regardless of the case, the module with a high figure of merit has a relatively high maximum output power. Similarly, regardless of the module, the filling of the metal foam significantly increases the maximum output power compared to the results of Case 0, with only a slight difference. For example, when the pore density is 40 PPI and the filling rate is 75% (Case 4), the output power of the thermoelectric generator using the KTGM161-18 module can be up to 35.5 W, and the maximum output power of the thermoelectric generator using the KTGM199-2 module is 31.2 W. These values are about 1.64 times and 1.44 times the maximum output power produced when the TEHP1-12656-0.3 module is used, respectively. This shows that for the condition of enhanced heat transfer, although the module with a high figure of merit can still achieve better thermoelectric conversion performance, the range by which it can be increased is reduced.

It can also be seen from fig. 5(b), for the TEHP1-12656-0.3 module in Cases 1 and 4, the maximum output power is increased by about 95% and 141%, respectively, compared to unfilled channel Case 0. For the KTGM199-2 module in the same cases, the maximum output power is increased by about 53% and 134%, respectively. Finally, for the KTGM161-18 module in the same cases, the maximum output power is increased by about 80% and 122%, respectively. Therefore, compared with the experimental results in [27], the high figure of merit module and enhanced heat transfer used in this paper can significantly improve the maximum output power of the thermoelectric generator.

Figure 6 shows the comparison of the power generation efficiency of the thermoelectric generator using three different thermoelectric modules with and without the metal foam. As shown in the figure, the thermoelectric conversion efficiency increases with the use of the high performance module and the enhancement of heat exchange. The magnitude of the efficiency increase caused by the module change is almost the same as the maximum power increase, but the magnitude of the efficiency increase caused by the heat transfer enhancement is lower than that of the maximum power output. This is because as the enhanced heat transfer increases, the temperature of the hot side of the thermoelectric generator increases, the temperature difference between the hot and cold sides of the thermoelectric module increases, and the output power increases. However, as the heat transfer is enhanced, the heat absorption at the hot side of the modules is also increased, so the amplitude of the increase in thermoelectric conversion efficiency is lower than that of in output power. For Cases 1, 2, and 3, the maximum power output and the thermoelectric conversion efficiency of the TEHP1-12656-0.3 and KTGM161-18 modules change only slightly with a given enhancement in heat transfer, while the gas-flow resistance of the latter two cases increases significantly. As shown in fig. 3(d), the friction coefficient of Case 4 is about four times that of Case 1, and the maximum output power of Case 4 is only 1.23 times that of Case 1 no matter which module is used. Therefore, considering the possible adverse effects of an increase in flow resistance, Case 1 is a good choice when using high performance modules.

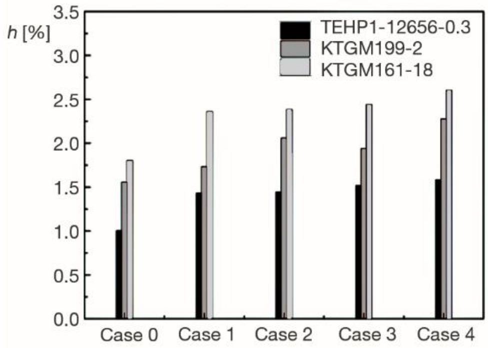

Figure 6. Comparison of efficiency of thermoelectric generator with three different modules

It can be seen from the previous experimental results, with the improvement of the performance of the thermoelectric module, the maximum output power and efficiency of the thermoelectric generator with the filling in the channel are greatly improved. For the Case 4 conditions, the maximum output power and efficiency of the thermoelectric generator using the KTGM161-18 module are 300% and 160% higher than those of the thermoelectric generator using the TEHP1-12656-0.3 module in the Case 0 conditions, respectively. This indicates that the combination of a thermoelectric module with a high figure of merit and an enhancement in heat transfer can greatly improve the output power and power generation efficiency, which is very important for the commercial application of thermoelectric generators.

Conclusions

In this paper, the effect of the enhancement of core flow heat transfer with metal foam on the performance of thermoelectric generators with different power generation characteristics was studied experimentally. The results show that.

- First, the heat transfer enhancement of partially filled metal foam in the core area of the gas channel can significantly improve the performance of the thermoelectric generator, which uses high temperature gas as the heat source and cooling water as the cold source. Although the pore density and filling rate of the foam metal were different, the maximum output power of the thermoelectric generator with TEHP1-12656-0.3 modules can be increased by 1.0-1.4 times.

- Second, for Case0, the thermoelectric generator using the KTGM161-18 module has the highest output power, and the TEHP1-12656-0.3 module has the lowest output power. The figures of merit for the KTGM161-18 and KTGM199-2 modules are about 2.5 and 2.1 times that of TEHP1-12656-0.3, respectively, and their maximum output powers are about 1.8 and 1.55 times that of TEHP1-12656-0.3, respectively. for Case 4, the output power of the thermoelectric generator using the KTGM161-18 module can be up to 35.5 W, and the maximum output power of the thermoelectric generator using the KTGM199-2 module is 31.2 W. These values are about 1.64 times and 1.44 times the maximum output power produced when the TEHP1-12656-0.3 module is used, respectively.
- Third, with the improvement of the performance of the thermoelectric module, the maximum output power and efficiency of the thermoelectric generator with the filling in the channel are greatly improved. For the Case 4 conditions, the maximum output power and efficiency of the thermoelectric generator using a high figure of merit module KTGM161-18 are 300% and 160% higher than those of the thermoelectric generator using a low figure of merit module TEHP1-12656-0.3 in the Case 0 conditions, respectively. Therefore, thermoelectric generator with an excellent thermoelectric conversion module is best suited to improve its performance through heat transfer enhancement, while a thermoelectric generator with low-performance module may not be suited to improve its performance.

Nomenclature

A – gas channel heat exchange area, [m^2]
c – gas specific heat, [kJkg^{-1}K^{-1}]
D – equivalent diameter, [m]
f – friction coefficient, [–]
h – heat-transfer coefficient, [Wm^{-2}K^{-1}]
L – gas channel length, [m]
$\dot{m}$ – gas mass flow, [kgs^{-1}]
Nu – Nusselt number, [–]
Re – Reynolds number, [–]
PEC – performance evaluation criteria, [–]
Δp – pressure drop, [Pa]
T_{in} – gas inlet temperatures, [°C]
T_{ou} – gas – outlet temperatures, [°C]
ΔT – temperature difference, [°C]
$\bar{t}_{\mathrm{w2}}$ – gas channel outside wall average temperature, [°C]
u – gas velocity, [ms^{-1}]

Greek symbols

δ – wall thickness, [m]
λ – channel wall thermal conductivity, [Wm^{-1}K^{-1}]
μ – gas viscosity, [Pa·s]
ρ – gas density, [kgm^{-3}]

References

[1] Hixon, J. D., Design Criteria and Tow Year Clinical Results of Pu238 Fuelled Demand Pacemaker, *Proceeding*, 7th IECER, San Diego, Cal., USA, 1972, pp.765-770
[2] Qiu, K., Hayden, A .C. S., A Natural-Gas-Fired Thermoelectric Power Generation System, *Journal of Electronic Materials*, *38* (2009), 7, pp. 1315-1319
[3] Killander, A., Bass, J. C., A Stove-Top Generator for Cold Areas, *Proceedings*, 15th International Conference on Thermoelectrics, IEEE, Pasadena, Ca., USA, 1996, pp. 390-393
[4] Rinehart, G. H., Design Characteristics and Fabrication of Radioisotope Heat Sources for Space Missions, *Progress in Nuclear Energy*, *39* (2001), 3, pp. 305-319
[5] Gurbuz, H., Ateş, D., A Numerical Study on Processes of Charge and Discharge of Latent Heat Energy Storage System Using RT27 Paraffin Wax for Exhaust Waste Heat Recovery in a SI Engine, *International Journal of Automotive Science And Technology*, *4* (2020), 4, pp. 314-327
[6] Gurbuz, H., Demirturk, S., Investigation of Dual-Fuel Combustion by Different Ort Injection Fuels (Neat Ethanol and E85) in a DE95 Diesel/Ethanol Blend Fuelled CI Engine, *Journal of Energy Resources Technology*, *142* (2020), 12, pp. 122306

[7] Gurbuz, H., *et al.*, Effect of Port Injection of Ethanol on Engine Performance, Exhaust Emissions and Environmental Factors in A Dual-Fuel Diesel Engine, *Energy and Environment*, *32* (2021), 5, pp. 784-802
[8] Gurbuz, H., *et al.*, Environmental and Enviroeconomic Assessment of an LPG Fueled SI Engine at Partial Load, *Journal of Environmental Management*, *241* (2019), July, pp. 631-636
[9] Topalci, U., *et al.*, Theoretical Optimization of the P-N Type Semiconductor Material Pair in Thermoelectric Generator that Achievement Exhaust Waste Heat Recovery, *Gazi University Journal of Science Part C: Design and Technology, 8* (2020), 3, pp. 588-600
[10] Ge, M., *et al.*, Experimental Study On Thermoelectric Power Generation Based on Cryogenic Liquid Cold Energy, *Energy*, *220* (2021), 6, 119746
[11] Jang, J. Y., Tsai, Y. C., Optimization of Thermoelectric Generator Module Spacing and Spreader Thickness Used in a Waste Heat Recovery System, *Applied Thermal Engineering*, *51* (2013), 1-2, pp. 677-689
[12] Liu, X., *et al*., Experiments and Simulations on Heat Exchangers in Thermoelectric Generator for Automotive Application, *Applied Thermal Engineering*, *71* (2014), 1, pp. 364-370
[13] Byung, I. D., *et al.*, The Study of a Thermoelectric Generator with Various Thermal Conditions of Exhaust Gas from a Diesel Engine, *International Journal of Heat and Mass Transfer*, *86* (2015), July, pp. 667-680
[14] Lu, X., *et al.*, Experimental Investigation On Thermoelectric Generator with Non-Uniform Hot-Side Heat Exchanger for Waste Heat Recovery, *Energy Conversion and Management*, *150* (2017), Oct., pp. 403-414
[15] Wang, Y., *et al.*, The Influence of Inner Topology of Exhaust Heat Exchanger and Thermoelectric Module Distribution on the Performance of Automotive Thermoelectric Generator, *Energy Conversion and Management*, *126* (2016), Oct., pp. 266-277
[16] Kim, T. Y., *et al.*, Direct Contact Thermoelectric Generator (DCTEG): A Concept for Removing the Contact Resistance Between Thermoelectric Modules and Heat Source, *Energy Conversion and Management*, *142* (2017), June, pp. 20-27
[17] Megerlin, F. E., *et al.*, Augmentation of Heat Transfer in Channels by Use of Mesh and Brush Inserts, *Journal of Heat Transfer*, *96* (1974), 2, pp. 145-151
[18] Wang, S., *et al*., Heat Transfer Enhancement by Using Metallic Filament Insert in Channel Flow, *International Journal of Heat & Mass Transfer*, *44* (2001), 7, pp. 1373-1378
[19] Pavel, B. I., Mohamad, A. A., An Experimental and Numerical Study on Heat Transfer Enhancement for Gas Heat Exchangers Fitted with Porous Media, *International Journal of Heat & Mass Transfer*, *47* (2004), 23, pp. 4939-4952
[20] Hsieh, W. H., *et al.*, Experimental Investigation of Heat-Transfer Characteristics of Aluminum-Foam Heat Sinks, *International Journal of Heat & Mass Transfer*, *47* (2004), 23, pp. 5149-5157
[21] Boomsma, K., *et al.*, Metal Foams as Compact High Performance Heat Exchangers, *Mechanics of Materials*, *35* (2003), 12, pp. 1161-1176
[22] Pavel, B. I., Mohamad, A. A., An Experimental and Numerical Study on Heat Transfer Enhancement for Gas Heat Exchangers Fitted with Porous Media, *International Journal of Heat & Mass Transfer*, *47* (2004), 23, pp. 4939-4952
[23] Mohamad, A. A., Heat Transfer Enhancements in Heat Exchangers Fitted with Porous Media Part I: Constant Wall Temperature, *International Journal of Thermal Sciences*, *42* (2003), 4, pp. 385-395
[24] Wei, L., Yang, K., Mechanism and Numerical Analysis of Heat Transfer Enhancement in the Core Flow Along a Channel, *Science China Technological Sciences*, *51* (2008), 8, pp. 1195-1202
[25] Huang, Z. F., *et al*., Enhancing Heat Transfer in the Core Flow by Using Porous Medium Insert in a Channel, *International Journal of Heat & Mass Transfer*, *53* (2010), 5-6, pp. 1164-1174
[26] Zheng, Z. J., *et al.*, Optimization of Porous Insert Configuration in a Central Receiver Channel for Heat Transfer Enhancement, *Energy Procedia*, *75* (2015), Aug., pp. 502-507
[27] Li, Y. Z., *et al.*, Experimental Study on the Influence of Porous Foam Metal Filled in the Core Flow Region on the Performance of Thermoelectric Generators, *Applied Energy*, *207* (2017), Dec., pp. 634-642
[28] Webb, R. L., Performance Evaluation Criteria for Use of Enhanced Heat Transfer Surfaces in Heat Exchanger Design, *International Journal of Heat & Mass Transfer*, *24* (1981), 4, pp. 715-726

Paper submitted: March 9, 2021
Paper revised: April 10, 2021
Paper accepted: April 17, 2021